JMEPEG (2017) 26:6057–6063
https://doi.org/10.1007/s11665-017-3042-7

1059-9495/$19.00

Corrosion Characteristics of New Superalloy Under Industrial Environmental Conditions

I.V.S. Yashwanth and I. Gurrappa

(Submitted March 31, 2017; in revised form September 21, 2017; published online November 1, 2017)

Corrosion behavior of new superalloy was studied in industrial environment at different temperatures by using various selected electrochemical techniques. The results revealed that the alloy is able to form protective oxide scale on its surface at higher temperatures and consequently the corrosion rate is low. The new alloy is found to degrade due to pitting corrosion at 40 and 50 °C and general corrosion at 25 °C. The scanning electron microscope results confirmed the electrochemical results. The energy-dispersive spectroscopy results confirmed the presence of oxides of nickel and alloying elements present in the superalloy. Based on the results obtained with different techniques, the alloy is recommended to fabricate different components for industrial applications with suitable protective coatings.

Keywords applications, corrosion characteristics, new superalloy

1. Introduction

Superalloys exhibit excellent mechanical strength, creep resistance and good surface stability over steels, which make them one of the alternatives for high-temperature applications (Ref 1). Due to their unique properties, nickel-based alloys are used for a variety of applications including gas turbines, chemical and petrochemical processing, pollution control, oil and gas extraction, marine engineering, power generation, pulp and paper manufacturing. The versatility and reliability of these alloys make them the prime materials of choice for process vessels, pumps, valves and many other applications used aqueous and high-temperature environments (Ref 2-5).

The new nickel-based superalloy which designated as DMS-31 was developed by Defence Metallurgical Research Laboratory (DMRL) for gas turbine engine applications. The corrosion resistance of superalloys depends on their chemistry such as nature of alloying elements and their concentration. Major change in the new superalloy is the addition of niobium and ruthenium. These are unique elements, which help to increase high-temperature creep properties considerably, but make the alloy susceptible to hot corrosion and high-temperature oxidation (Ref 6). It is due to the fact that the superalloy cannot form stable and protective alumina or chromia scale because of the presence of rhenium and ruthenium. However, some Ni-based superalloys exhibit good corrosion resistance in aqueous environments at ambient temperatures (Ref 7, 8). For obtaining higher efficiencies, the components of industrial systems have to be fabricated from materials which satisfy both mechanical as well as corrosion resistance. It is pertinent to note that corrosion determines the life of components in a variety of industries. Therefore, materials selection based on their corrosion resistance enhances the efficiency, reduces down time, which in turn improves their production and consequently profitability (Ref 9-14).

Gurrappa and his group studied the hot corrosion and oxidation of different nickel-based superalloys extensively at various temperatures and developed smart coatings to enhance the efficiency of gas turbines significantly (Ref 9-12). Gaona-Tiburcio et al. (Ref 7) reported the corrosion behavior of Inconel 690, 718, Incoloy 800 and 825 in 10% H_2SO_4 and 10% CH_3COOH at room temperature by electrochemical noise technique. The corrosion resistance in H_2SO_4 environment was reported in the following order: Inconel 800 < Inconel 690 < Inconel 718 < Inconel 825, while in CH_3COOH environment, the order was Inconel 718 < Inconel 800 < Inconel 825 < Inconel 690. Mohammed et al. (Ref 8) studied the behavior of Inconel 718 alloy with and without rhenium (2.4, 3.5, 6 wt.%) in 1.0 M H_2SO_4, 0.1 M, 0.3 M and 0.6 M NaCl at 25 °C by using various electrochemical techniques. Open-circuit potential (OCP) studies revealed that the tested alloys tend to passivate in H_2SO_4 solutions, and the extent of passivation depends on rhenium content. The passivation rate was reported to increase in the following order: IN718-6%Re < IN718 < IN718-2.4%Re < IN718-3.5%Re. The lowest passivation rate was reported for IN718-6% Re among the tested alloys, indicating its active corrosion surface when compared to IN718. The corrosion behavior of other superalloys at ambient temperature was also reported (Ref 15-18). However, the literature contains few studies about the corrosion and anodic behavior of superalloys at ambient temperatures.

The present investigation is aimed at studying the corrosion behavior of DMS-31 superalloy in simulated industrial environment at different temperatures with a view to understand its corrosion characteristics and subsequently to recommend for fabrication of components intended to use in different industries.

2. Experimental

The chemical composition of new superalloy is presented in Table 1. The test specimens of 3 mm thick and 14 mm in

I.V.S. Yashwanth, Department of Metallurgical and Materials Engineering, University of Texas at El Paso, El Paso, TX, USA; and **I. Gurrappa**, Defence Metallurgical Research Laboratory, Kanchanbagh PO, Hyderabad 500 058, India. Contact e-mail: igp1@rediffmail.com.

Table 1 Nominal composition of new superalloy (wt.%, Ni-Balance)

Cr	Co	Mo	W	Ta	Al	C	Ru	Re	Hf	Nb
7.0	10	2.0	6.0	9.0	5.6	0.02	2.0	1.0	0.1	1.2

diameter were prepared from the homogenized cylindrical superalloy rods following casting. The specimens were then grounded up to 800 grit surface finish, cleaned with distilled water followed by acetone.

The corrosion behavior of DMS-31 was studied in 0.5 M solution of 90% Na_2SO_4 and 10% NaCl (simulated industrial environment) at different temperatures such as 25, 40, and 50 °C by using CHI680C potentiostat (CH Instruments, Inc.USA) with exposed surface area of 1 cm^2. Open-circuit potential versus time, electrochemical noise, AC impedance, potentiodynamic and cyclic polarization techniques were used to understand the corrosion characteristics of new superalloy. The open-circuit potential versus time curves were used to assess the protective nature of the superalloy. Potentiodynamic polarization technique was used to determine the active/passive characteristics of the alloy-solution system and to determine the corrosion rates. AC impedance curves were used to understand solution and polarization resistance. Electrochemical noise measurements and cyclic polarization techniques were used to evaluate the pitting and crevice corrosion resistance of new superalloy in the industrial environment at different temperatures. Finally, scanning electron microscopy (SEM) was used to understand the degradation mechanism of the alloy and energy-dispersive spectroscopy (EDS) to determine the corrosion products that were formed during exposure to industrial environment at various temperatures.

3. Results

3.1 Open-Circuit Potential Versus Time

The variation of open-circuit potential as a function of time for DMS-31 in industrial environment at temperatures of 25, 40 and 50 °C is shown in Fig. 1. As can be seen, the potential of new superalloy is shifted toward positive side initially and then moved slightly negative side at 40 °C. It indicates that protective oxide scale is formed on the surface of DMS-31 alloy and subsequently started dissolving. At 50 and 25 °C, the alloy maintains a steady potential with time indicating that the film remains intact and protective. Generally, a rise of potential in the positive direction indicates the formation of the passive film and a steady potential indicates that the film remains intact and protective. A drop of potential in the negative direction indicates breaks in the film, dissolution of the film or no film formation. Therefore, any alloy for obtaining good corrosion resistance, the potentials should either shift to more positive side or maintain a steady value as a function of time under the chosen environmental conditions. The present results show that the alloy did not form a protective oxide scale for its corrosion resistance at 40 °C but forms stable and protective oxide scale at 50 and 25 °C in industrial environment.

3.2 Electrochemical Noise Measurements

The results obtained by industrial solution on DMS-31 alloy at different temperatures come from analyzing the time series of current noise to determine the electrochemical noise resistance (R_n). There are constant frequencies and amplitude transients causing the superalloy to undergo general corrosion at 25 °C, while at 40 and 50 °C, there are high frequencies and amplitude transients causing the superalloy to undergo pitting corrosion. Any corrosion process that is uniform over a metal surface is associated with constant fluctuations because of reaction with the environment over the entire exposed alloy surface, whereas the localized corrosion process causes high fluctuations in corrosion current as a function of time due to selective corrosion of certain precipitates or phases. The current transients with time are known to be closely associated with the initiation and repassivation which provides useful information on the type of corrosion. Figure 2 shows that there are constant frequencies and amplitude transients, causing that the alloy is undergone uniform corrosion at 25 °C and pitting corrosion at 40 and 50 °C.

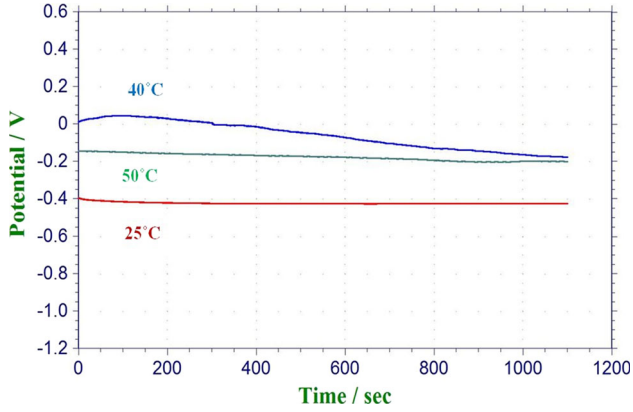

Fig. 1 Open-circuit potential of DMS-31 superalloy at different temperatures as a function of time in industrial environment

3.3 AC Impedance Measurements

AC impedance offers further confirmation to the extent of surface reactivity of DMS-31 under open-circuit conditions in industrial environment. The low-frequency capability has led to probe and readily detects relaxation phenomena involving surface intermediates and thus studying electrochemical corrosion and passivation mechanisms. Prior to the impedance scan, each specimen was left immersed in the test solution until a steady-state open-circuit potential was reached. All measurements were taken in the frequency domain 0.01 Hz-1 MHz. AC impedance measurements for DMS-31 in industrial environment at different temperatures are shown in Fig. 3. DMS-31 superalloy exhibits high impedance characteristics at 50 and 40 °C. The significantly reduced impedance recorded at 25 °C for DMS-31 afforded markedly faster charge transfer process that occurred on the alloy surface. The Nyquist plots allow a more effective extrapolation of data from higher frequencies (Fig. 3b). Phase versus log (freq) showed that the corrosion resistance of DMS-31 is high at higher temperatures when compared to ambient temperature (Fig. 3c).

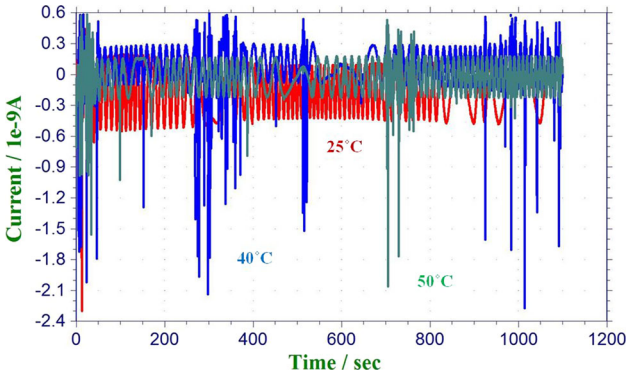

Fig. 2 Electrochemical noise measurements for DMS-31 superalloy at different temperatures in industrial environment

3.4 Cyclic Polarization Measurements

The cyclic polarization curves for DMS-31 in industrial environment at different temperatures are shown in Fig. 4. At 25 °C, reverse scan came above the forward scan indicating that the alloy is not susceptible to pitting corrosion. While at 50 and 40 °C, the reverse scan came below the forward scan indicating that the alloy is susceptible to pitting and crevice corrosion. Generally, the behavior of any alloy under the testing conditions can be adjudged by observing the loop formation, i.e., if the alloy reverse scan comes below the forward scan and forms loop, then the alloy is susceptible to pitting corrosion. Otherwise, if the reverse scan comes above the forward scan and forms no loop, the alloy is resistant to pitting corrosion. Again, it is important to observe the loop area during the experiment. More is the loop area, higher is the susceptibility and less is the area, less vulnerable to pitting. The technique also helps to compare different alloys under the simulated conditions to compare their susceptibility to pitting by comparing the loop areas. Further, the intersection of forward and reverse scans provides the information regarding the susceptibility to crevice corrosion. In the present study, the alloy is resistant to pitting and crevice corrosion at 25 °C and degraded due to general corrosion, while at 40 and 50 °C, the alloy degraded due to pitting and crevice corrosion. It is to be noted that the alloy is more susceptible to pitting corrosion at 40 °C when compared to 50 °C as the formed loop area is large.

3.5 Potentiodynamic Polarization Measurements

Corrosion potential (E_{corr}), corrosion current density (I_{corr}), anodic, cathodic Tafel slopes and corrosion rates were measured for DMS-31 in the industrial environment at 25, 40, 50 °C (Fig. 5) and presented in Table 2. The corrosion potential at 25 °C is more cathodic when compared to 40 and 50 °C. Similarly the corrosion current density of DMS-31 at 25 °C is higher than the corrosion current density at 40 °C and 50 °C. The current density at 25 °C is about three and half times higher than that of current density at 40 °C and about three times than that of current density at 50 °C. Consequently, the corrosion rate at 25 °C is higher than the corrosion rate at 40 and 50 °C. In essence, minimum corrosion rate is observed at 40 °C, increases marginally at 50 °C and maximum at 25 °C.

3.6 Surface Morphology Studies

With a view to confirm the corrosion mechanism of new superalloy at various temperatures in industrial environment, all

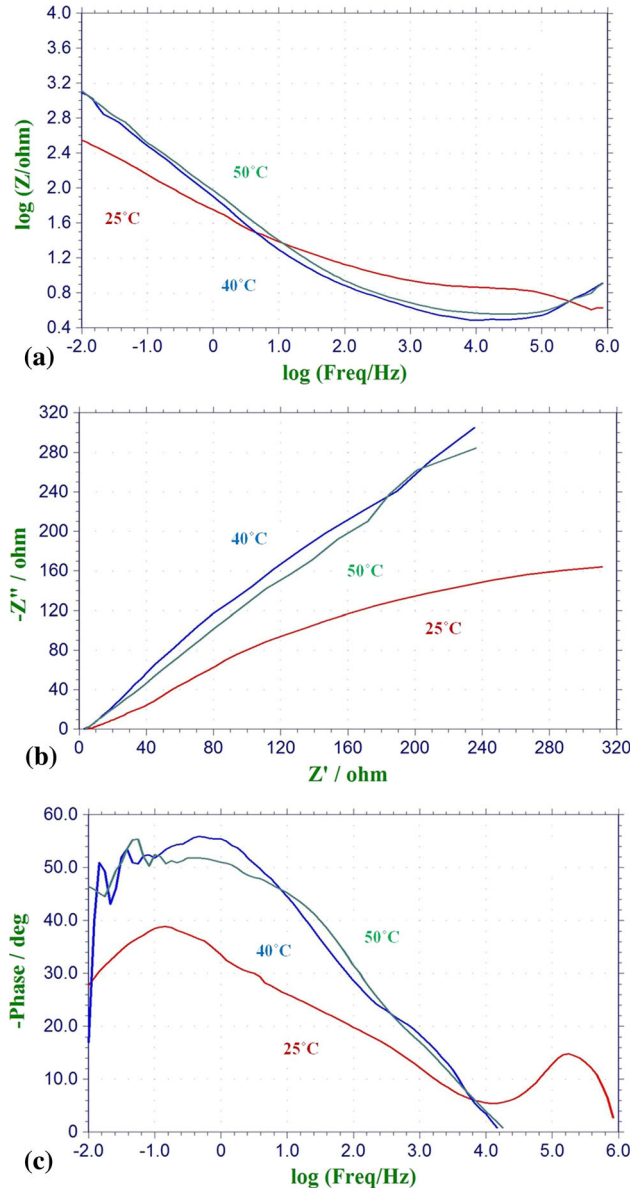

Fig. 3 AC impedance measurements for DMS-31 superalloy at different temperatures in industrial environment (a) Bodo plots (b) Nyquist plots (c) phase angle

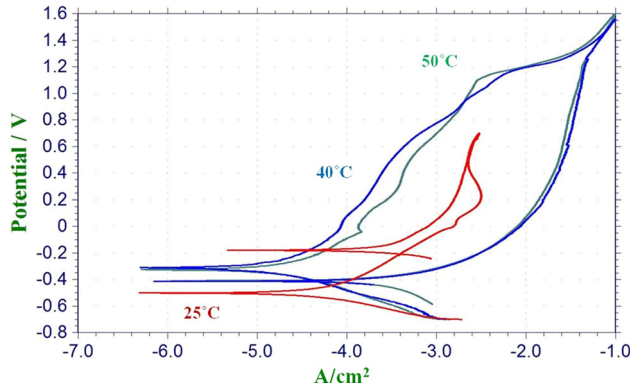

Fig. 4 Cyclic polarization plots for DMS-31 superalloy at different temperatures in industrial environment

corroded specimens were observed under scanning electron microscope. As can be seen from the surface morphologies (Fig. 6), the alloy was corroded due to general corrosion at 25 °C. It is also clear that the alloy corrosion rate is very high at 25 °C, formed thick oxide scale which subsequently cracked. While at 40 and 50 °C, the alloy was corroded at localized sites confirming that the new superalloy was corroded because of pitting corrosion. Thus, the surface morphologies are in agreement with cyclic polarization results (Fig. 4).

3.7 Energy Dispersive Spectroscopy (EDS)

Energy-dispersive spectroscopic patterns of new superalloy that were collected from rectangular regions (Fig. 6) at various temperatures in industrial environment are shown in Fig. 7. The data revealed that the peaks are corresponding to base metal, i.e., nickel, all the alloying elements present in the alloy and oxygen. However, the intensity of peaks varied from one temperature to another. The results are indicating that the superalloy forms oxides of nickel and all the alloying elements during the corrosion process. The findings are in agreement with the results obtained at elevated temperatures under hot corrosion conditions (Ref 19).

Typical EDS data of new superalloy at 50 °C are presented in Table 3. The results revealed that the major amount of oxide is nickel followed by tungsten and tantalum. Other oxides of alloying elements are low. It is pertinent to note that aluminum and chromium oxide contents are low and nearly same. It indicates that nickel and tungsten followed by tantalum are more reactive with the industrial environment and thus causing degradation of the new superalloy.

4. Discussion

It is a general practice to choose the material which exhibits low corrosion rate in the given environmental conditions in association with appropriate protective coatings for fabrication of components for any application/system. It is also important to consider the construction material along with selected coatings that should be tested under simulated environmental conditions before introducing into the service as corrosion is catastrophic in nature and responsible for disasters during service. It is pertinent to mention that Inconel 718 superalloy is widely used in marine applications as fasteners and hardware as

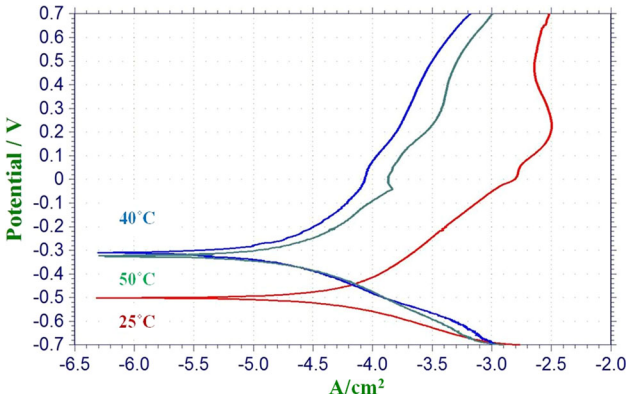

Fig. 5 Potentiodynamic polarization results for DMS-31 superalloy at different temperatures in industrial environment

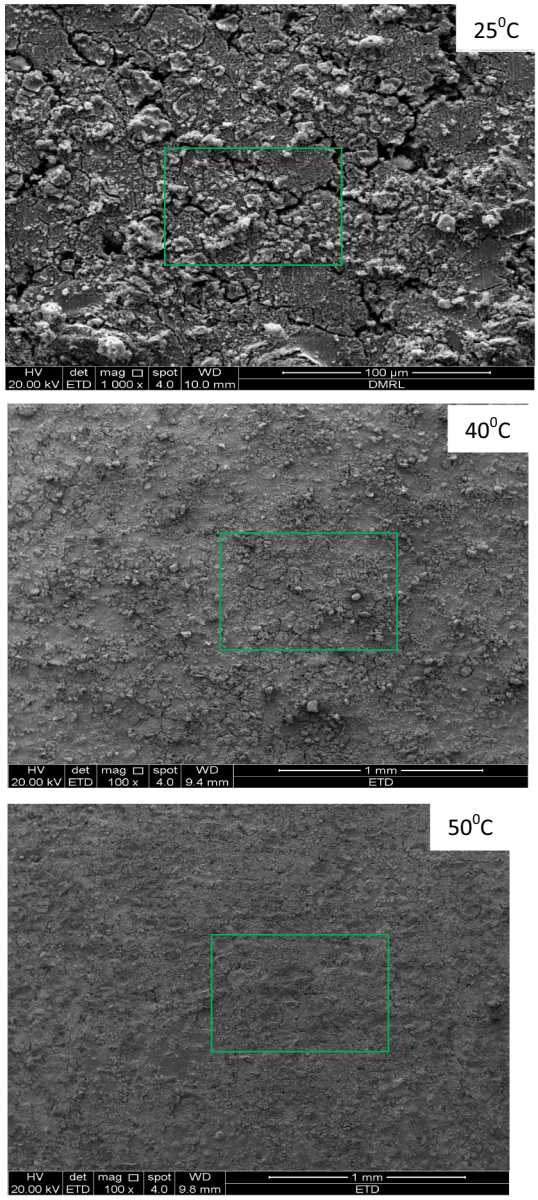

Fig. 6 Surface morphologies of DMS-31 superalloy at different temperatures in industrial environment and squares are the EDS collected data

Table 2 Electrochemical results of DMS-31 superalloy in industrial environment at various temperatures

Temperature, °C	I_{corr}, μA/cm^2	E_{corr}, V	Cathodic slope	Anodic slope	Corrosion rate, mils/year
25	50.89	− 0.501	7.234	4.416	26.99
40	14.71	− 0.309	6.369	4.313	7.803
50	18.36	− 0.322	6.180	4.574	9.737

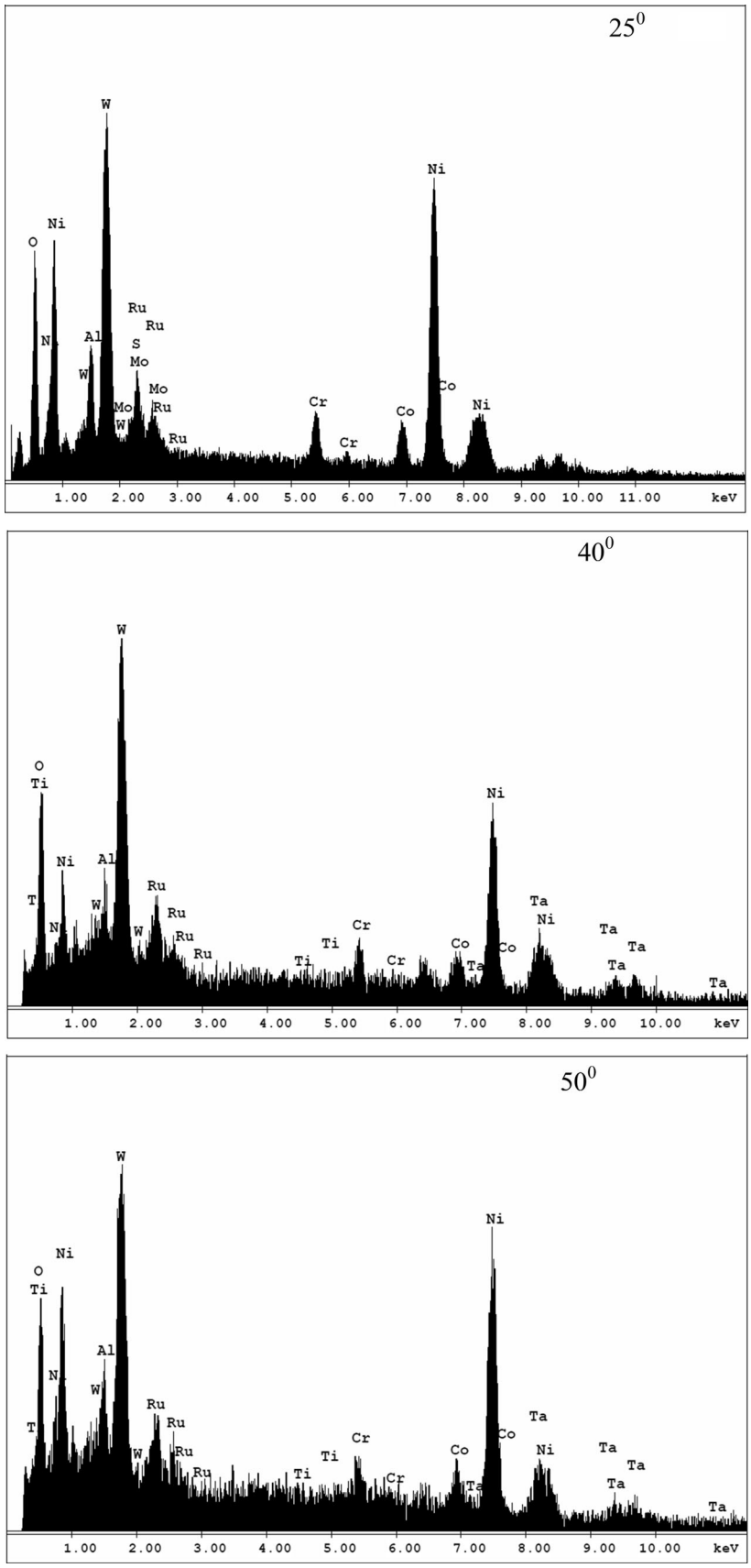

Fig. 7 EDS patterns of corroded DMS-31 superalloy in industrial environment at various temperatures

Table 3 Typical EDS data of corroded DMS-31 superalloy in industrial environment at 50 °C

Element	wt.%	at.%
Oxygen	12.10	42.42
Aluminum	2.94	6.11
Titanium	0.77	0.90
Ruthenium	3.09	1.72
Chromium	2.79	3.01
Cobalt	4.17	3.97
Nickel	29.49	28.17
Tantalum	17.29	5.36
Tungsten	27.35	4.78

it exhibits good corrosion resistance in seawater due to the formation of protective oxide (Ref 8, 20-22). Therefore, nickel-based superalloys exhibit unusual corrosion resistance in many corrosive environments. However, certain aggressive ions like Cl^-, Br^- can induce passivity breakdown resulting in localized corrosion and stress corrosion cracking (Ref 17, 23-26). Acid environment can also result in corrosion attack thus leading to premature failure. Hence, as mentioned earlier, selection of materials based on their corrosion resistance in selected environmental conditions is essentially needed. Thus, considering the potential applications of new superalloy and due to aggressive environments where such alloys are intended to be used, the requirement is to have not only high tensile and creep strength but also high corrosion resistance. Thus, the corrosion resistance of new superalloy DMS-31 in industrial, marine and acid environments is an important issue to study and hence detailed corrosion studies were undertaken in industrial environment containing aggressive sulfur and chloride ions, which are normally present in the industrial region. The results in other environments will be published elsewhere. Further, the temperature in the industrial areas is varying from 25 to 50 °C. During the operation of industrial units, the temperature is able to reach about 50 °C. Further, the industrial environment contains sulfur and chloride ions. Hence, the temperatures and the environment chosen in the present study are relevant to industrial environmental conditions.

The present results revealed that the new superalloy DMS-31 exhibits minimum corrosion rate in the simulated industrial environment at 40 °C, increased slightly when the temperature increased to 50 and maximum corrosion rate was reached at 25 °C. Further, the alloy showed maximum polarization resistance at high temperature when compared to lower temperatures. However, appropriate surface engineering treatment is needed as the passive film (chromia and alumina) does not afford complete protection for the superalloy as evidenced from the results. The literature revealed that Inconol 718 superalloy undergoes pitting corrosion in marine environment due to breakdown of passive film. The industrial environment that contains chloride ions makes the new superalloy to undergo pitting corrosion. Thus, the literature supports the present results. Further, it was reported that superalloys exhibit low corrosion rate in different environments when compared to carbon and stainless steels under similar environmental conditions (Ref 7). The new superalloy exhibits excellent mechanical properties and maximum oxidation resistance even under high-temperature applications such as gas turbine engine components (Ref 6). Therefore, it is recommended to use DMS-31 superalloy for fabrication of components used for industrial applications with suitable surface engineering treatment.

5. Conclusions

The new superalloy exhibits minimum corrosion rate in industrial environment when compared to carbon and stainless steels. It undergoes pitting corrosion at 40 and 50 °C and general corrosion at 25 °C. As the protective oxides that form on the new superalloy are not able to afford complete protection, appropriate surface engineering treatment is required. Therefore, it is recommended that DMS-31 superalloy is suitable to fabricate the components for industrial applications with suitable surface engineering treatment.

References

1. I. Gurrappa, I.V.S. Yashwanth, and A.K. Gogia, The Behaviour of Superalloys in Marine Gas Turbine Engine Conditions, *J. Surf. Eng. Mater. Adv. Technol.*, 2011, **1**, p 45
2. K. Fulton, Gas Turbine World, June 1994, p 52–56
3. M. Konter and M. Thumann, Materials and Manufacturing of Advanced Industrial Gas Turbine Components, *J. Mater. Proces. Technol.*, 2001, **117**, p 386
4. P. Caron and T. Khan, Evolution of Ni-Base Superalloys for Single Crystal Gas Turbine Blade Applications, *Aerosp. Sci. Technol.*, 1999, **3**, p 513
5. R. Hashizume, A. Yoshinari, T. Kiyono,Y. Murata, and M. Morinaga, Development of Ni-Based Single Crystal Superalloys for Power Generation Gas Turbines, Superalloys 2004, p 53–62
6. I.V.S. Yashwanth, I. Gurrappa, and H. Murakami, Oxidation Behavior of a Newly Developed Superalloy, *J. Surf. Eng. Mater. Adv. Technol.*, 2011, **3**, p 130
7. C. Gaona-Tiburcio, L.M.R. Anguilar, P.Z. Robledo, F.E. Lopez, J.A.C. Mirmonates, D. Nieves-Mendoza, E. Castillo-Gonzalez, and F. Almeraya-Calderon, Electrochemical Noise Analysis of Nickel Based Superalloys in Acid Solutions, *Intl. J. Electrochem. Sci.*, 2014, **9**, p 523
8. M.A. Amin, N. El-Bagoury, M. Saracoglu, and M. Ramadan, Electrochemical and Corrosion Behaviour of Cast Re-containing Inconel 718 Alloys in Sulphuric Acid Solutions and the Effect of Cl^-, *Int. J. Electrochem. Sci.*, 2014, **9**, p 5352
9. I. Gurrappa, Hot Corrosion Behavior of CM 247 LC Alloy in Na_2SO_4 and NaCl Environments, *Oxid. Metals*, 1999, **51**, p 353
10. I. Gurrappa, Identification of Hot Corrosion Resistant MCrAlY Based Bond Coatings for Gas Turbine Engine Applications, *Surf. Coat. Technol.*, 2001, **139**, p 272
11. I. Gurrappa, I.V.S. Yashwanth, and A.K. Gogia, The selection of materials for marine gas turbines, Gas Turbines ISBN:979-953-307-816-7, Volkov Konstarton (Editor), INTECH Publishers, 2012, p 51–70
12. I. Gurrappa and I.V.S. Yashwanth, *Design and Development of Smart Coatings for Gas Turbines. "Gas Turbines"*, ed. by I. Gurrappa. ISBN: 978-953-307-146-6, SCIYO Publishers, 2010, p 65–78
13. C.J. Wang and J.H. Lin, The Oxidation of MAR M 247 Superalloy with Na_2SO_4 Coating, *Chem. Phys.*, 2002, **76**, p 123
14. J.R. Nicholls, N.J. Simms, W.Y. Chan, and H.E. Evans, Smart coatings-Concept and Practice, *Surf. Coat. Technol.*, 2001, **149**, p 236
15. T. Nickechi and A. Alfantazi, Electrochemical Corrosion Behavior of Incoloy 800 in Sulphate Solutions Containing Hydrogen Peroxide, *Corr. Sci.*, 2010, **52**, p 4035
16. N.K. Aylikci, E. Tirabsoglu, I.H. Karahan, V. Aylikci, M. Eskil, and E. Cengiz, Alloying Effect on KX-Ray Intensity Ratios, KX-Ray Production Cross-Sections and Radiative Augur Ratios in Superalloys

Constitute from Al, Ni and Mo Elements, *Chem. Phys.*, 2010, **377**, p 100

17. T. Chen, H. John, J. Xu, Q. Lu, J. Hawk, and X. Liu, Influence of Surface Modifications on Pitting Corrosion Behavior of Nickel Base Superalloy 718, *Corr. Sci.*, 2013, **77**, p 230
18. W. Batista, A.M.T. Louvisse, O.R. Mattos, and L. Sathler, The Electrochemical Behavior of INCOLOY 800 and AISI, 304 Steel in Solutions that are Similar to Those Within Occluded Corrosion Cells, *Corros. Sci.*, 1988, **28**, p 759
19. I. Gurrappa, I.V.S. Yashwanth, I. Mounika, H. Murakami, and S. Kuroda, "*The importance of hot corrosion of Superalloys and their effective Protection for Enhanced Efficiency of Gas Turbine Engines. Gas Turbines, Materials, Modelling and Performance*", ed. by I. Gurrappa. ISBN:978-953-51-1743-8, INTECH Publishers, 2015, p 55–102
20. H.J. Jang, C.J. Park, and H.S. Kwon, Photoelectrochemical Analysis on the Passive Film Formed on Ni in pH 8.5 Buffer Solution, *Electrochim. Acta*, 2005, **50**, p 3503
21. N. Pineau, C. Minot, V. Maurice, and P. Marcus, Density Functional Theory Study of the Interaction of Cl- with Passivated Nickel Surfaces, *Electrochem. Solid-State Lett.*, 2003, **6**, p B47
22. A. Bouzoubaa, B. Diawara, V. Maurice, C. Minot, and P. Marcus, Ab Initio Modelling of Localised Corrosion: Study of the Role of Surface Steps in the Interaction of Chlorides with Passivated Nickel Surfaces, *Corros. Sci.*, 2009, **51**, p 2174
23. F.R. Caliari, E.F. da Rosa, M.A. Silva, and D.A.P. Reis, Analysis of Pitting Corrosion on an Inconel 718 Alloy Submitted to Aging Heat Treatment, *Technol. Metal Mater. Miner.*, 2014, **11**, p 189
24. G.S. Frankel, Pitting Corrosion of Metals: A Review of the Critical Factors, *J. Electrochem. Soc.*, 1998, **145**, p 2186
25. K.V. Rybalka, L.A. Beketaeva, and A.D. Davydov, Effect of Self-Passivation on the Electrochemical and Corrosion Behavior of Alloy C-22 in NaCl Solution, *Corros. Sci.*, 2012, **54**, p 161
26. D.D. Macdonald, Theoretical Investigation of the Evolution of the Passive State on Alloy 22 in Acidified, Saturated Brine Under Open Circuit Conditions, *Electrochim. Acta*, 2011, **56**, p 7411